

Functional Reconstitution of the Na⁺-driven Polar Flagellar Motor Component of *Vibrio alginolyticus**

(Received for publication, October 27, 1999, and in revised form, November 30, 1999)

Ken Sato‡ and Michio Homma

From the Division of Biological Science, Graduate School of Science, Nagoya University, Chikusa-ku, Nagoya 464-8602, Japan

The bacterial flagellar motor is a molecular machine that couples the influx of specific ions to the generation of the force necessary to drive rotation of the flagellar filament. Four integral membrane proteins, PomA, PomB, MotX, and MotY, have been suggested to be directly involved in torque generation of the Na⁺-driven polar flagellar motor of *Vibrio alginolyticus*. In the present study, we report the isolation of the functional component of the torque-generating unit. The purified protein complex appears to consist of PomA and PomB and contains neither MotX nor MotY. The PomA/B protein, reconstituted into proteoliposomes, catalyzed ²²Na⁺ influx in response to a potassium diffusion potential. Sodium uptake was abolished by the presence of Li⁺ ions and phenamil, a sodium channel blocker. This is the first demonstration of a purification and functional reconstitution of the bacterial flagellar motor component involved in torque generation. In addition, this study demonstrates that the Na⁺-driven motor component, PomA and PomB, forms the Na⁺-conducting channel.

Flagella are the filamentous organelles responsible for bacterial motility. Flagellar rotation is driven by a reversible rotary motor embedded in the cytoplasmic membrane at the base of each flagellar filament (1–3). Energy for rotation of the flagellar motor comes from the transmembrane electrochemical potential of specific ions. Two types of motors, proton-driven (2) and sodium-driven (4), dependent on different coupling ions, have been described. The proton-driven motors of *Escherichia coli* and *Salmonella typhimurium* have been extensively studied, and the stator part of the torque generator consists of two cytoplasmic membrane proteins, MotA and MotB, which contain four transmembrane domains and one transmembrane domain, respectively (5–8). Much genetic and physiological evidence suggests that MotA and MotB together form a proton channel (9–13), and this complex is believed to be anchored to the cell wall via the peptidoglycan-binding domain of MotB (8, 14, 15). Ions passing through these proteins are thought to generate torque (16), which is transmitted to the rotor part of the motor, the FliG protein (17, 18). FliG forms a complex together with FliM and FliN (19, 20) called the “switch complex,” which is essential for torque generation, flagellar assembly, and control of the direction of motor rotation (21–23).

Bacteria such as alkalophilic *Bacillus* and *Vibrio* species use an electrochemical gradient of sodium to drive flagellar rota-

tion (4). The sodium-driven motor has advantages for the study of motor function because sodium-motive force can be easily manipulated. The specific sodium channel blockers, amiloride and phenamil, are powerful tools for studying the mechanism of energy conversion in this system (24, 25). Four proteins essential for torque generation, PomA, PomB, MotX, and MotY, were recently identified in the polar flagellar motor of *Vibrio alginolyticus* (26, 27). PomA and PomB are homologous to MotA and MotB and contain four transmembrane segments and one transmembrane segment, respectively. MotX and MotY, first identified in *Vibrio parahaemolyticus* (28, 29), have a single putative transmembrane domain that is unique to the sodium-type motor. MotY has a peptidoglycan-binding motif at the carboxyl-terminal region that is also observed in MotB and PomB. Evidence suggests that MotX is part of the sodium channel component of the motor. Overexpression of MotX is lethal to *E. coli* in proportion to the external sodium ion concentration. Lethality is reversed in the presence of amiloride (29). Although the above four components are thought to form a sodium channel, no direct evidence has been demonstrated so far.

In the present study, we report the isolation and reconstitution of the torque-generating unit of the Na⁺-driven polar flagellar motor component of *V. alginolyticus* as a stage in its biochemical characterization. The complex, purified via His-tagged PomA, includes both PomA and PomB and has an approximate molecular size of 175 kDa. In addition, reconstituted PomA/B proteoliposomes exhibit potassium diffusion potential-driven ²²Na⁺ uptake that is blocked by Li⁺ ions and phenamil. These results suggest that the heteromultimeric complex, consisting of PomA and PomB, acts as a sodium channel that generates the torque to drive flagellar rotation.

MATERIALS AND METHODS

Bacterial Strains, Plasmids, Growth Conditions, and Media—*V. alginolyticus* strains NMB190 (Rif^r, Pof⁺, Laf⁻, Δ*pomA*) (30) and NMB191 (Rif^r, Pof⁺, Laf⁻, Δ*pomA*, Δ*pomB*) (31) were used and cultured at 30 °C in VC medium (0.5% (w/v) polypeptone, 0.5% (w/v) yeast extract, 0.4% (w/v) K₂HPO₄, 3% (w/v) NaCl, 0.2% (w/v) glucose) or VPG medium (1% (w/v) polypeptone, 0.4% (w/v) K₂HPO₄, 3% (w/v) NaCl, 0.5% (w/v) glycerol). For the swarm assay, a VPG/0.3% agar plate was used. *E. coli* strain JM109 (*recAI*, *endAI*, *gyrA96*, *thi*⁻, *hsdR17*, *relAI*, *supE44*, λ⁻, Δ(*lac-proAB*); *F*['], *traD36*, *proAB*, *lacI*^q, Δ*M15*) was used for DNA manipulations and cultured at 37 °C in LB medium. When necessary, kanamycin was added to a final concentration of 100 μg/ml for *Vibrio* cells or 25 μg/ml for *E. coli* cells. Plasmid pKS101, a pSU41-based plasmid, was constructed to carry *his₆pomA* under the *lac* promoter control. A 0.8-kilobase DNA fragment including the *pomA* open reading frame with a 5' attachment of 5'-ATTGGATCCATGCATCAC-CATCACCATCACATGGATTTAGCAACCTATTA-3' (initiates as Met-His₆; the underline indicates the created (*Bam*HI and *Eco*T22I) restriction sites) was originally prepared by polymerase chain reaction and cloned into *Bam*HI-digested pSU41. Plasmid pKS105, encoding the tandem PomA, was generated by engineering an *Eco*T22I site at the 3' end of the *pomA* clone, and then linked to the 5' end of *his₆pomA* via *Eco*T22I. The final linking sequence was Met-His₆ (one methionine and

* This study was supported by grants from the Ministry of Education, Science, Sports and Culture of Japan. The costs of publication of this article were defrayed in part by the payment of page charges. This article must therefore be hereby marked “advertisement” in accordance with 18 U.S.C. Section 1734 solely to indicate this fact.

‡ To whom correspondence should be addressed: Tel.: 81-52-789-2992; Fax: 81-52-789-3001; E-mail: m47004a@nucc.cc.nagoya-u.ac.jp.

six histidines), which was added at the junction. All the total inserts were confirmed by DNA sequencing.

Purification of PomA/B Complex—Cells of NMB190 harboring pKS101 were cultured at 30 °C under strong aeration in VPG medium. Cells were harvested and washed with buffer (20 mM Tris-Cl, pH 8.0, 5 mM MgSO₄, 10% (w/v) sucrose) and stored at -80 °C until use. The frozen cells were thawed, resuspended (0.2 g/ml, wet weight) in 20 mM Tris-Cl, pH 8.0, containing 1 mM dithiothreitol, 5 mM MgSO₄, 30 µg/ml DNase I, and 0.5 mM phenylmethylsulfonyl fluoride. Membrane vesicles were prepared by subjecting the suspension to a single passage through a French press (5501-M Ohtake Works) at 4000 p.s.i. at 4 °C. Undisrupted cells were removed by low speed centrifugation (10,000 × g for 20 min at 4 °C), and the membrane fraction was recovered from the supernatant by centrifugation at 200,000 × g for 2 h. The membrane pellet was suspended in Buffer A (20 mM Tris-Cl, pH 8.0, 150 mM NaCl, 1 mM dithiothreitol, 0.5 mM phenylmethylsulfonyl fluoride, 20% (w/v) glycerol) containing 5 mM imidazole, pH 8.0, and 2.5% (w/v) β-octylglucoside. The suspension was stirred for 30 min at room temperature and centrifuged for 20 min at 10,000 × g. The clarified extract was mixed with Ni-NTA¹-agarose (Qiagen) prewashed with the same buffer, incubated at 4 °C for 1 h with gentle mixing, and then packed into the column. The loaded resin was washed with Buffer A containing 40 mM imidazole, pH 8.0, and 1.25% (w/v) β-octylglucoside. Elution was conducted with Buffer A containing 500 mM imidazole, pH 8.0, and 1.25% (w/v) β-octylglucoside. The Ni-NTA-purified material was diluted 5-fold with Buffer B (20 mM Tris-Cl, pH 8.0, 20% (w/v) glycerol, 1.25% (w/v) β-octylglucoside) and applied to a MiniQ column (Amersham Pharmacia Biotech) equilibrated with Buffer B. The column was washed with Buffer B, and bound material was eluted with a 0–800 mM linear gradient of KCl in Buffer B. Fractions were analyzed by immunoblotting with anti-PomB antibody. Peak fractions were combined and concentrated by a MiniQ column. PomA/B complex was eluted from the column at a salt concentration of ~220 mM. The concentrated solution was applied on a Superose 6 gel filtration column (Amersham Pharmacia Biotech) equilibrated with Buffer B containing 100 mM KCl. The peak fractions containing both His₆-PomA and PomB were pooled and stored at -80 °C. Purification of His₆-PomA alone from NMB191 (*ΔpomAB*) strain harboring pKS101 was performed essentially as described above. Protein concentrations were assayed by the BCA protein assay reagent (Pierce).

Reconstitution of Proteoliposomes—Proteoliposomes were reconstituted by the octylglucoside dilution method. A sample of purified PomA/B complex (8.0 µg) or His₆-PomA (4.7 µg) was mixed with 5.0 mg of *E. coli* phospholipids (Avanti Polar Lipids) in 20 mM Tris-Cl, pH 8.0, 200 mM KCl, 1.25% (w/v) β-octylglucoside, 10% (w/v) glycerol. The mixture (100 µl) was sonicated briefly, incubated on ice for 20 min, and rapidly diluted (40-fold) into the dilution buffer (20 mM Tris-Cl, pH 8.0, 200 mM KCl). After 15 min at room temperature with gentle shaking, the proteoliposomes formed were recovered by centrifugation at 200,000 × g for 1 h, resuspended in 100 µl of dilution buffer, frozen in dry ice/ethanol, and stored at -80 °C. When assayed, the suspension was thawed at room temperature.

Orientation of the PomA/B Complex in the Proteoliposomes—Inverted membrane vesicles were prepared as described above. Preparation of spheroplasts of *V. alginolyticus* was performed as described previously (44). Membranes (60 µl) were treated with 15 µl of Proteinase K at the indicated concentrations on ice for 30 min. The samples were precipitated with trichloroacetic acid, washed with acetone, and then analyzed by SDS-PAGE, followed by immunoblotting with anti-PomB antibody (31).

Determination of ²²Na⁺ Uptake by Proteoliposomes—The standard incubation mixture contained 500 µl of the following at 30 °C: 20 mM Tris-Cl, pH 8.0, 200 mM choline chloride, 0.5 mM ²²NaCl (4 µCi/ml), and proteoliposomes loaded with 200 mM KCl (50 µl). The mixture was allowed to equilibrate for 5 min. Inhibitors were added, and after a 1-min incubation, a membrane potential was applied by adding 20 µM valinomycin. At intervals, 90 µl of the reaction mixture was filtered through a nitrocellulose filter (0.2-µm pore size, Toyo Roshi Co. Ltd.) with suction and washed three times with 1 ml of 20 mM Tris-Cl buffer, pH 8.0, containing 200 mM choline chloride. The radioactivity trapped on the filter was determined by a γ-counter.

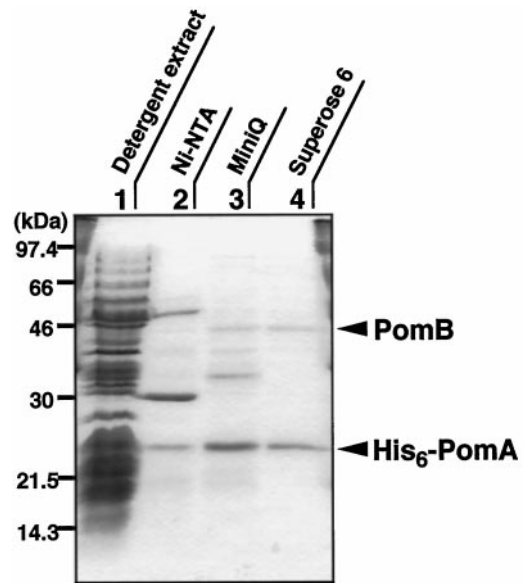


FIG. 1. Purification of the torque-generating unit. The protein pattern at the different stages of the purification procedure is visualized by 15% SDS-PAGE and by staining with Coomassie Brilliant Blue. Lane 1, detergent extract (45 µg) of *V. alginolyticus* membrane; lane 2, eluant resulting from the membrane fraction subjected to Ni-NTA chromatography (20 µg); lane 3, further purification by MiniQ anion exchange chromatography (11 µg); lane 4, combined eluant fractions containing both PomA and PomB after Superose 6 chromatography (9 µg).

RESULTS

Isolation of the Torque-generating Unit of the Polar Flagellar Motor from *V. alginolyticus*—We isolated the torque-generating unit of the polar flagellar motor from *V. alginolyticus* based on the features characterized for PomA protein; at least it forms a functional complex with PomB protein in the cytoplasmic membrane (31). We constructed a plasmid, pKS101, that encodes PomA with an attached hexahistidine sequence on the amino terminus of the protein, His₆-PomA. The plasmid, pKS101, complemented a *pomA* null mutant; these results were similar to those observed with pYA301, which encodes wild-type PomA. In addition, the swimming speed of the cells harboring pKS101 was similar to that of wild-type cells (data not shown). Thus, the attachment of the hexahistidine tag does not interfere with PomA function. Membrane fractions of NMB190 transformed with pKS101 were prepared, solubilized with β-octylglucoside (Fig. 1, lane 1), and passed through a Ni-NTA-agarose column. The agarose column was washed, and bound protein was eluted with the buffer containing imidazole (Fig. 1, lane 2). The eluate from the Ni-NTA-agarose resin was applied to a MiniQ anion exchange column and eluted with a salt gradient. The eluate was analyzed by immunoblots using antibodies generated against PomA and PomB, and fractions that contained both PomA and PomB were collected (Fig. 1, lane 3). Finally, using a Superose 6 column, most other proteins were quantitatively removed, and PomA was eluted together with PomB but not with either MotX or MotY (Fig. 1, lane 4). Although His₆-PomA is overexpressed in the cells, the protein complex purified above contains only endogenous PomB. Coomassie Brilliant Blue staining intensities of PomA and PomB bands of the complex separated by SDS-PAGE were measured by densitometry. The ratio of bound dye was 1.0:0.55 (PomA: PomB), and taking the molecular size of each protein into account, a calculated ratio of PomA and PomB in the complex was found to be 2.3:1.0 (PomA:PomB). Thus, it seems that the apparent molar ratio of PomA/B in the purified complex is 2

¹ The abbreviations used are: NTA, nitrilotriacetic acid; PAGE, polyacrylamide gel electrophoresis.

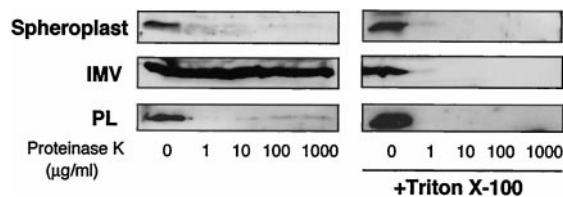


FIG. 2. **Orientation of PomA/B in cells and liposomes.** Treatment of spheroplasts, inverted membrane vesicles (IMV) from NMB190 ($\Delta pomA$) cells harboring pKS101, and proteoliposomes (PL) with Proteinase K was performed as described under "Materials and Methods." As controls, spheroplasts, inverted membrane vesicles, and proteoliposomes were lysed with Triton X-100 before the protease treatment. Immunoblot was done with antibody generated against the carboxyl-terminal epitope of PomB. Samples that had not been treated with Proteinase K were also examined.

PomA:1 PomB, although the exact estimation necessitates more detailed investigation.

Reconstitution of the PomA/B Complex into Proteoliposomes—Proteoliposomes were prepared from purified PomA/B and *E. coli* phospholipids by the detergent dilution method (32, 33). To assess whether the PomA/B complex was properly reconstituted in the liposomes, we compared its topological orientation in liposomes to that of PomA/B in spheroplasts (Fig. 2). Treatment of spheroplasts with Proteinase K cleaved the carboxyl-terminal epitope of PomB. The same cleavage occurred after purified PomA/B complex inserted into liposomes was treated with Proteinase K. The carboxyl-terminal epitope of PomB in inverted membrane vesicles was protected from Proteinase K digestion by the membranes. However, lysis by Triton X-100 of spheroplasts, inverted membrane vesicles, or proteoliposomes resulted in carboxyl-terminal digestion by Proteinase K. A quantitative assessment of the PomB digestion in spheroplasts and proteoliposomes indicates that at least 80–90% of the purified PomA/B was inserted into liposomes with the correct orientation (right side out). We conclude that the purified PomA/B complexes that were incorporated into liposomes were asymmetrically inserted with the same relative orientation as in the cytoplasmic membrane.

$^{22}\text{Na}^+$ Transport into Reconstituted Proteoliposomes—The kinetics of $^{22}\text{Na}^+$ uptake into reconstituted proteoliposomes are shown in Fig. 3. When valinomycin was added to potassium-loaded PomA/B liposomes, creating $\Delta\psi$ in response to the potassium gradient, $^{22}\text{Na}^+$ was rapidly translocated to the inside of proteoliposomes. No significant $^{22}\text{Na}^+$ uptake was observed in control liposomes without PomA/B (data not shown) or PomB, indicating that the PomA/B complex but not valinomycin is responsible for $^{22}\text{Na}^+$ translocation. If the driving force for sodium uptake consisted of only $\Delta p\text{Na}^+$, the rate of $^{22}\text{Na}^+$ uptake was very low. These results are indicative of an electrogenic Na^+ transport by purified PomA/B complex. The accumulation of $^{22}\text{Na}^+$ ions was effectively prevented by the presence of 50 μM phenamil, which is a specific inhibitor of the sodium-driven flagellar motor (25, 34).

The sodium-driven motor of *V. alginolyticus* has been shown to function using lithium ion (35). Sodium translocation into PomA/B proteoliposomes was effectively inhibited by Li^+ , indicating that Na^+ and Li^+ compete at a common binding site on the protein. These results are the first clear evidence of a bacterial flagellar motor component that acts directly as a primary ion channel.

Molecular Properties of the PomA/B Complex—To determine the apparent molecular size of the PomA/B complex, we performed gel permeation chromatography by loading purified PomA/B complex along with several molecular mass standards onto a Superose 6 column. The PomA/B complex was eluted between catalase (240 kDa) and aldolase (158 kDa) (Fig. 4).

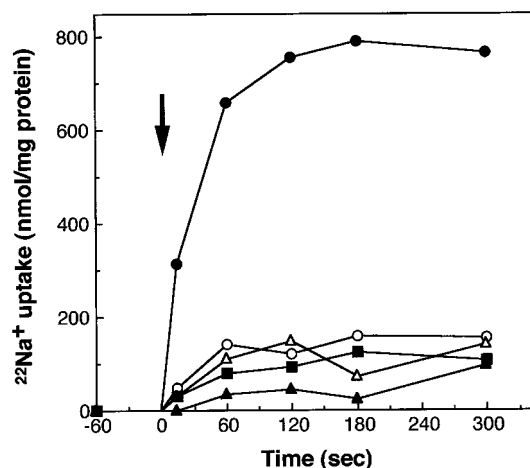


FIG. 3. **Kinetics of $^{22}\text{Na}^+$ uptake into reconstituted proteoliposomes containing PomA/B and effect of inhibitors.** $\Delta\psi$ was created as a K^+ diffusion potential by adding valinomycin to KCl-loaded proteoliposomes. The uptake of $^{22}\text{Na}^+$ ions was determined in incubation mixtures containing the proteoliposomes (2.5 mg of lipids) in a total volume of 0.5 ml. The addition of valinomycin is marked by the arrow (filled circles). Parallel experiments were performed with incubation mixtures containing 50 μM phenamil (open circles), 10 mM LiCl (open triangles), and proteoliposomes containing His₆-PomA (filled squares). Also shown is a control without valinomycin (filled triangles). Uptake experiments were carried out more than five times, and typical data are shown.

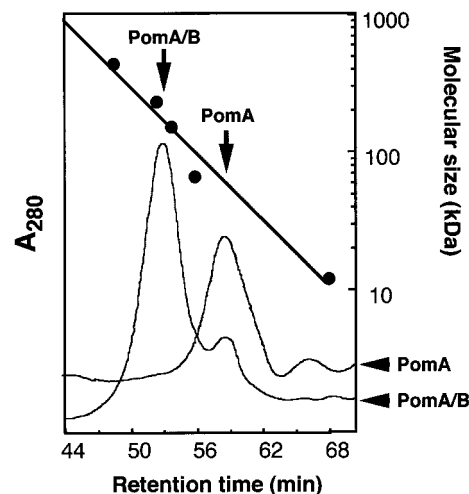


FIG. 4. **Molecular size of PomA/B complex and PomA estimated from Superose 6 chromatography.** The purified PomA/B complex or His₆-PomA was loaded on a Superose 6 column equilibrated with 20 mM Tris-Cl buffer, pH 8.0, containing 100 mM KCl and 20% (w/v) glycerol and eluted at a flow rate of 0.03 ml/min. The molecular size standards used are ferritin (450 kDa), catalase (240 kDa), aldolase (158 kDa), albumin (68 kDa), and cytochrome *c* (12.5 kDa). The arrows indicate the position of the retention time of PomA/B (PomA/B) complex and His₆-PomA (PomA).

Considering the micellar size of β -octylglucoside (2.1 kDa), the apparent molecular size of the PomA/B complex was estimated to be 175 kDa.

We further purified His₆-PomA alone from a *pomAB* null mutant strain (NMB191) harboring pKS101. When purified His₆-PomA was applied to the Superose 6 column as described above, His₆-PomA was eluted faster than would be expected for the PomA monomer (Fig. 4), which has a molecular size of 27 kDa. The estimated molecular size was 55 kDa. This result suggests that PomA alone exists as a stable homodimer in detergent extract.

To further elucidate the dimeric structure of PomA, we con-

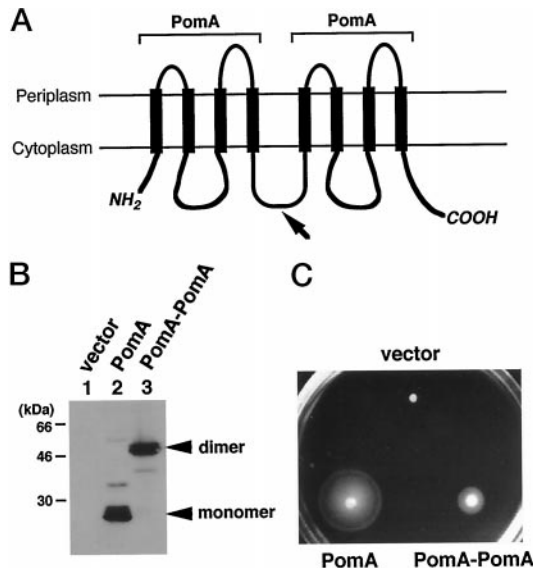


FIG. 5. Expression and function of tandem PomA. A, schematic diagram of a PomA-PomA dimer. Two PomA monomers joined tail-to-head in tandem are expressed as a single polypeptide. The arrow indicates the position of the connecting site, and the linking sequence is Met-His₆. B, membrane vesicles (10 μ g of protein each) of NMB190 ($\Delta pomA$) harboring a vector plasmid (lane 1), a plasmid encoding His₆-PomA (lane 2), or tandem PomA (lane 3) were subjected to SDS-PAGE and immunoblotting with anti-PomA antibody. C, swarming abilities of NMB190 ($\Delta pomA$) cells expressing no PomA (vector), His₆-PomA (PomA), or tandem PomA (PomA-PomA). Overnight cultures were spotted on VPG/0.3% agar plates containing kanamycin and incubated at 30 °C.

structed a plasmid encoding tandems of two PomA subunits expressed as a single polypeptide (Fig. 5A). Previous studies suggested that PomA has four membrane spans and that the amino and carboxyl termini must be on the same side of the membrane (26). Hence a tandem complex of two covalently linked PomA subunits might be expected to assemble into a functional state. The construction was performed by linking two *pomA* open reading frames in frame with six histidines as a linker. As shown in Fig. 5C, NMB190 ($\Delta pomA$) cells expressing the tandem PomA did indeed show ability to swarm in a soft agar plate. Compared with wild-type PomA, NMB190 cells expressing tandem PomA demonstrated a reduction in swarming ability. Since the carboxyl terminus of *Salmonella* MotA has been shown to be important for its activity (36), diminished swarm ability may be due to restricted flexibility around the carboxyl terminus of the amino-terminal half of tandem PomA. To demonstrate that the swarm activity observed is due to the activity of full-length tandem PomA and not to monomeric PomA, either from partial translation or proteolytic degradation of PomA fusion, immunoblots were prepared using membrane preparations from NMB190 expressing the tandem fusion protein. As shown in Fig. 5B, tandem PomA migrates at around 50 kDa. It should be noted that no other immunoreactive species is observed on the immunoblots, particularly around 25 kDa, where the monomeric His₆-PomA migrates. The functional tandem fusion PomA was purified by Ni-NTA resin from the NMB191 ($\Delta pomAB$) strain that expresses tandem PomA by Ni-NTA resin. The molecular size was analyzed by a Superose 6 column together with Ni-NTA-purified monomeric His₆-PomA, and the fractions were examined by immunoblotting with anti-PomA antibody. The purified His₆-PomA was eluted in exactly the same fractions as tandem PomA (Fig. 6). These results strongly support the stable homodimerization of native PomA.

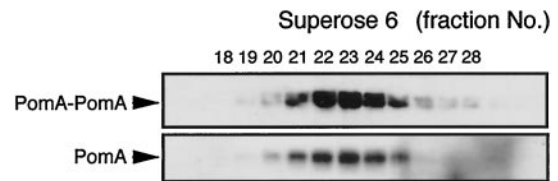


FIG. 6. Size exclusion chromatography of His₆-PomA (PomA) and tandem PomA (PomA-PomA) on a Superose 6 column. His₆-PomA and tandem PomA were briefly purified by a Ni-NTA column and then applied to a Superose 6 column. The anti-PomA immunoblot profile of each fraction is shown.

DISCUSSION

We have reconstituted the flagellar motor component of *V. alginolyticus* into proteoliposomes from pure phospholipids and purified membrane protein. Our results indicate that the purified PomA/B complex forms a sodium-conducting channel, whereas purified PomA alone does not. Although we have not examined the ability of PomB alone to mediate ²²Na⁺ translocation, PomB has been shown to be degraded in the absence of PomA, and the simultaneous expression of both PomA and PomB is required for the stability of PomB (31). MotX and MotY, which are also essential components required for torque generation *in vivo*, are apparently not part of the complex. Our data, however, do not exclude the possibility of a further stimulatory effect on sodium transport by MotX and MotY, or MotX and MotY might form a sodium channel independent of the PomA/B complex that may even be essential for torque generation. The isolation of the MotX and MotY proteins is now in progress and should help to clarify the function of those components. Can we exclude the possibility that minor contaminants contribute to or even cause the activities ascribed to the PomA/B complex? On the basis of sodium uptake activity per unit amount of PomA/B complex, proteoliposomes reconstituted from the PomA/B complex, which was purified from the strains overexpressing both His₆-PomA and PomB, were as active as those reconstituted from the His₆-PomA-overproducing strain (data not shown), suggesting that PomA and PomB were enough to catalyze sodium uptake.

Even though the functional partnership of PomA and PomB proteins, as well as *E. coli* MotA and MotB, has been established, information concerning their interactions and molecular stoichiometry is very limited. Indeed, their physical interaction has been demonstrated so far only by a co-sedimentation analysis (31, 37). An important finding in this study is that the Na⁺-driven flagellar motor components of *V. alginolyticus*, PomA and PomB, are purified as a functional complex. The subunit ratio of purified complex was estimated to be 2 PomA:1 PomB, which is about 89 kDa in size. Considering that the apparent molecular size of the PomA/B complex was 175 kDa, the native functional complex might consist of four copies of PomA and two copies of PomB as a single torque-generating unit, although more detailed investigation is required. When the purified His₆-PomA alone was applied to a Superose 6 column, His₆-PomA was eluted as a stable homodimer, suggesting that an even number of PomA subunits is recruited per functional complex. Consistent with the presence of homodimeric PomA, when the purified PomA/B complex was analyzed by a Superose 6 column, the elution profile showed two peaks corresponding to the PomA/B complex and to dimeric PomA, which may be dissociated from the complex.

PomA/B reconstituted into liposomes facilitates Na⁺ uptake in a phenamil-sensitive manner. This finding is consistent with our previous observation that phenamil interacts directly with PomA/B (34) and with the closely related bacterium *V. parahaemolyticus* (38). The present study also shows that Na⁺ uptake was abolished with the presence of Li⁺ ions. This result is

in good agreement with previous results suggesting that lithium can substitute for sodium (35). These observations further underscore the complexity of PomA/B pore selectivity. Interestingly, $^{22}\text{Na}^+$ uptake appears to be directed by the membrane potential but not by the concentration gradient. This result suggests that the transport of Na^+ ions through the PomA/B complex is an electrogenic event. At present, however, the importance of this channel property in regard to torque generation remains unclear. The mechanism linking the translocation of $\Delta\psi$ -driven Na^+ ions across the motor component to the generation of rotary torque for flagellar rotation may be similar to the proposed voltage-generated torque generation of the Na^+ -translocating F_1F_0 -ATPase of *Propionigenium modestum* (39).

Complex membrane events, such as solute transport (40), subreactions of oxidative phosphorylation, protein translocation in bacteria (41, 42) and the endoplasmic reticulum (43), and the membrane fusion step of trafficking (33), have been functionally reconstituted into proteoliposomes, thus allowing the direct investigation of fundamental cell biological mechanisms. This study demonstrates the availability of a pure, functional flagellar motor component, which can be reconstituted into proteoliposomes able to catalyze ion transport, as an avenue toward the enzymological resolution of torque generation.

Acknowledgment—We thank Dr. Ikuro Kawagishi for critically reading the manuscript.

REFERENCES

- Berg, H. C. (1995) *Biophys. J.* **68**, (suppl.) 163–167
- Blair, D. F. (1995) *Annu. Rev. Microbiol.* **49**, 489–522
- DeRosier, D. J. (1998) *Cell* **93**, 17–20
- Imae, Y., and Atsumi, T. (1989) *J. Bioenerg. Biomembr.* **21**, 705–716
- Dean, G. E., Macnab, R. M., Stader, J., Matsumura, P., and Burks, C. (1984) *J. Bacteriol.* **159**, 991–999
- Stader, J., Matsumura, P., Vacante, D., Dean, G. E., and Macnab, R. M. (1986) *J. Bacteriol.* **166**, 244–252
- Zhou, J. D., Fazio, R. T., and Blair, D. F. (1995) *J. Mol. Biol.* **251**, 237–242
- Chun, S. Y., and Parkinson, J. S. (1988) *Science* **239**, 276–278
- Blair, D. F., and Berg, H. C. (1990) *Cell* **60**, 439–449
- Stolz, B., and Berg, H. C. (1991) *J. Bacteriol.* **173**, 7033–7037
- Sharp, L. L., Zhou, J. D., and Blair, D. F. (1995) *Biochemistry* **34**, 9166–9171
- Garza, A. G., Harrishaller, L. W., Stoebner, R. A., and Manson, M. D. (1995) *Proc. Natl. Acad. Sci. U. S. A.* **92**, 1970–1974
- Garza, A. G., Biran, R., Wohlschlegel, J. A., and Manson, M. D. (1996) *J. Mol. Biol.* **258**, 270–285
- Blair, D. F., Kim, D. Y., and Berg, H. C. (1991) *J. Bacteriol.* **173**, 4049–4055
- De Mot, R., and Vanderleyden, J. (1994) *Mol. Microbiol.* **12**, 333–334
- Meister, M., Lowe, G., and Berg, H. C. (1987) *Cell* **49**, 643–650
- Lloyd, S. A., Tang, H., Wang, X., Billings, S., and Blair, D. F. (1996) *J. Bacteriol.* **178**, 223–231
- Zhou, J. D., Lloyd, S. A., and Blair, D. F. (1998) *Proc. Natl. Acad. Sci. U. S. A.* **95**, 6436–6441
- Francis, N. R., Sosinsky, G. E., Thomas, D., and Derosier, D. J. (1994) *J. Mol. Biol.* **235**, 1261–1270
- Oosawa, K., Ueno, T., and Aizawa, S. (1994) *J. Bacteriol.* **176**, 3683–3691
- Yamaguchi, S., Fujita, H., Ishihara, H., Aizawa, S., and Macnab, R. M. (1986) *J. Bacteriol.* **166**, 187–193
- Socketk, H., Yamaguchi, S., Kihara, M., Irikura, V., and Macnab, R. M. (1992) *J. Bacteriol.* **174**, 793–806
- Irikura, V. M., Kihara, M., Yamaguchi, S., Socketk, H., and Macnab, R. M. (1993) *J. Bacteriol.* **175**, 802–810
- Sugiyama, S., Cragoe, E. J., Jr., and Imae, Y. (1988) *J. Biol. Chem.* **263**, 8215–8219
- Atsumi, T., Sugiyama, S., Cragoe, E. J., Jr., and Imae, Y. (1990) *J. Bacteriol.* **172**, 1634–1639
- Asai, Y., Kojima, S., Kato, H., Nishioka, N., Kawagishi, I., and Homma, M. (1997) *J. Bacteriol.* **179**, 5104–5110
- Okunishi, I., Kawagishi, I., and Homma, M. (1996) *J. Bacteriol.* **178**, 2409–2415
- McCarter, L. L. (1994) *J. Bacteriol.* **176**, 4219–4225
- McCarter, L. L. (1994) *J. Bacteriol.* **176**, 5988–5998
- Asai, Y., Kawagishi, I., Socketk, R. E., and Homma, M. (1999) *J. Bacteriol.* **181**, 6332–6338
- Yorimitsu, T., Sato, K., Asai, Y., Kawagishi, I., and Homma, M. (1999) *J. Bacteriol.* **181**, 5103–5106
- Racker, E., Violand, B., O'Neal, S., Alfonzo, M., and Telford, J. (1979) *Arch. Biochem. Biophys.* **198**, 470–477
- Sato, K., and Wickner, W. (1998) *Science* **281**, 700–702
- Kojima, S., Asai, Y., Atsumi, T., Kawagishi, I., and Homma, M. (1999) *J. Mol. Biol.* **285**, 1537–1547
- Liu, J. Z., Dapice, M., and Khan, S. (1990) *J. Bacteriol.* **172**, 55236–55244
- Muramoto, K., and Macnab, R. M. (1998) *Mol. Microbiol.* **29**, 1191–1202
- Tang, H., Braun, T. F., and Blair, D. F. (1996) *J. Mol. Biol.* **261**, 209–221
- Jaques, S., Kim, Y. K., and McCarter, L. L. (1999) *Proc. Natl. Acad. Sci. U. S. A.* **96**, 5740–5745
- Kaim, G., and Dimroth, P. (1998) *EMBO J.* **17**, 5887–5895
- Kaback, H. R. (1988) *Annu. Rev. Physiol.* **50**, 243–256
- Brundage, L., Hendrick, J. P., Schiebel, E., Driessen, A. J. M., and Wickner, W. (1990) *Cell* **62**, 649–657
- Akimaru, J., Matsuyama, S., Tokuda, H., and Mizushima, S. (1991) *Proc. Natl. Acad. Sci. U. S. A.* **88**, 6545–6549
- Görlich, G., and Rapoport, T. A. (1993) *Cell* **75**, 615–630
- Osborn, M. J., and Munson, R. (1974) *Methods Enzymol.* **31**, 642–653